Search for an invisibly decaying Higgs boson in e^+e^- collisions at 189 GeV

R. Barate, D. Decamp, P. Ghez, C. Goy, S. Jezequel, J P. Lees, F. Martin, E. Merle, M N. Minard, B. Pietrzyk, et al.

EUROPEAN LABORATORY FOR PARTICLE PHYSICS (CERN)

CERN-EP/99-125

16 Sept 1999

Search for an invisibly decaying Higgs boson in e^+e^- collisions at 189 GeV

The ALEPH Collaboration[†]

Abstract

The data collected in 1998 by ALEPH at LEP at a centre-of-mass energy of 188.6 GeV, corresponding to an integrated luminosity of 176.2 pb^{-1}, are analysed to search for invisible decays of a Higgs boson produced in the reaction $e^+e^- \to hZ$. The number of events found in the data and their properties are in agreement with the Standard Model expectation. This search results in an improved 95% C.L. lower limit on the Higgs boson mass of 95.4 GeV/c^2, assuming it decays totally invisibly and for a production cross section equal to that of the Standard Model.

(Submitted to Physics Letters B)

[†]) See next pages for the list of authors

The ALEPH Collaboration

R. Barate, D. Decamp, P. Ghez, C. Goy, S. Jezequel, J.-P. Lees, F. Martin, E. Merle, M.-N. Minard, B. Pietrzyk

Laboratoire de Physique des Particules (LAPP), IN^{2}P^3-CNRS, F-74019 Annecy-le-Vieux Cedex, France

R. Alemany, S. Bravo, M.P. Casado, M. Chmeissani, J.M. Crespo, E. Fernandez, M. Fernandez-Bosman, Ll. Garrido,[15] E. Graugès, A. Juste, M. Martinez, G. Merino, R. Miquel, Ll.M. Mir, P. Morawitz, A. Pacheco, I. Riu, H. Ruiz

Institut de Física d'Altes Energies, Universitat Autònoma de Barcelona, 08193 Bellaterra (Barcelona), E-Spain[7]

A. Colaleo, D. Creanza, M. de Palma, G. Iaselli, G. Maggi, M. Maggi, S. Nuzzo, A. Ranieri, G. Raso, F. Ruggieri, G. Selvaggi, L. Silvestris, P. Tempesta, A. Tricomi,[3] G. Zito

Dipartimento di Fisica, INFN Sezione di Bari, I-70126 Bari, Italy

X. Huang, J. Lin, Q. Ouyang, T. Wang, Y. Xie, R. Xu, S. Xue, J. Zhang, L. Zhang, W. Zhao

Institute of High-Energy Physics, Academia Sinica, Beijing, The People's Republic of China[8]

D. Abbaneo, U. Becker,[19] G. Boix,[6] O. Buchmüller, M. Cattaneo, F. Cerutti, V. Ciulli, G. Dissertori, H. Drevermann, R.W. Forty, M. Frank, F. Gianotti, T.C. Greening, A.W. Halley, J.B. Hansen, J. Harvey, P. Janot, B. Jost, I. Lehraus, O. Leroy, P. Maley, P. Mato, A. Minten, A. Moutoussi, F. Ranjard, L. Rolandi, D. Schlatter, M. Schmitt,[20] O. Schneider,[2] P. Spagnolo, W. Tejessy, F. Teubert, E. Tournefier, A.E. Wright

European Laboratory for Particle Physics (CERN), CH-1211 Geneva 23, Switzerland

Z. Ajaltouni, F. Badaud G. Chazelle, O. Deschamps, S. Dessagne, A. Falvard, C. Ferdi, P. Gay, C. Guicheney, P. Henrard, J. Jousset, B. Michel, S. Monteil, J-C. Montret, D. Pallin, P. Perret, F. Podlyski

Laboratoire de Physique Corpusculaire, Université Blaise Pascal, IN^{2}P^3-CNRS, Clermont-Ferrand, F-63177 Aubière, France

J.D. Hansen, J.R. Hansen, P.H. Hansen, B.S. Nilsson, B. Rensch, A. Wäänänen

Niels Bohr Institute, 2100 Copenhagen, DK-Denmark[9]

G. Daskalakis, A. Kyriakis, C. Markou, E. Simopoulou, A. Vayaki

Nuclear Research Center Demokritos (NRCD), GR-15310 Attiki, Greece

A. Blondel, J.-C. Brient, F. Machefert, A. Rougé, M. Swynghedauw, R. Tanaka, A. Valassi,[23] H. Videau

Laboratoire de Physique Nucléaire et des Hautes Energies, Ecole Polytechnique, IN^{2}P^3-CNRS, F-91128 Palaiseau Cedex, France

E. Focardi, G. Parrini, K. Zachariadou

Dipartimento di Fisica, Università di Firenze, INFN Sezione di Firenze, I-50125 Firenze, Italy

M. Corden, C. Georgiopoulos

Supercomputer Computations Research Institute, Florida State University, Tallahassee, FL 32306-4052, USA [13,14]

A. Antonelli, G. Bencivenni, G. Bologna,[4] F. Bossi, P. Campana, G. Capon, V. Chiarella, P. Laurelli, G. Mannocchi,[1,5] F. Murtas, G.P. Murtas, L. Passalacqua, M. Pepe-Altarelli

Laboratori Nazionali dell'INFN (LNF-INFN), I-00044 Frascati, Italy

M. Chalmers, L. Curtis, J.G. Lynch, P. Negus, V. O'Shea, B. Raeven, C. Raine, D. Smith, P. Teixeira-

Dias, A.S. Thompson, J.J. Ward

Department of Physics and Astronomy, University of Glasgow, Glasgow G12 8QQ,United Kingdom[10]

R. Cavanaugh, S. Dhamotharan, C. Geweniger,[1] P. Hanke, V. Hepp, E.E. Kluge, A. Putzer, K. Tittel, S. Werner,[19] M. Wunsch[19]

Institut für Hochenergiephysik, Universität Heidelberg, D-69120 Heidelberg, Germany[16]

R. Beuselinck, D.M. Binnie, W. Cameron, P.J. Dornan,[1] M. Girone, S. Goodsir, N. Marinelli, E.B. Martin, J. Nash, J. Nowell, H. Przysiezniak, A. Sciabà, J.K. Sedgbeer, E. Thomson, M.D. Williams

Department of Physics, Imperial College, London SW7 2BZ, United Kingdom[10]

V.M. Ghete, P. Girtler, E. Kneringer, D. Kuhn, G. Rudolph

Institut für Experimentalphysik, Universität Innsbruck, A-6020 Innsbruck, Austria[18]

C.K. Bowdery, P.G. Buck, G. Ellis, A.J. Finch, F. Foster, G. Hughes, R.W.L. Jones, N.A. Robertson, M. Smizanska, M.I. Williams

Department of Physics, University of Lancaster, Lancaster LA1 4YB, United Kingdom[10]

I. Giehl, F. Hölldorfer, K. Jakobs, K. Kleinknecht, M. Kröcker, A.-S. Müller, H.-A. Nürnberger, G. Quast, B. Renk, E. Rohne, H.-G. Sander, S. Schmeling, H. Wachsmuth C. Zeitnitz, T. Ziegler

Institut für Physik, Universität Mainz, D-55099 Mainz, Germany[16]

J.J. Aubert, A. Bonissent, J. Carr, P. Coyle, A. Ealet, D. Fouchez, A. Tilquin

Centre de Physique des Particules, Faculté des Sciences de Luminy, IN^{2}P^3-CNRS, F-13288 Marseille, France

M. Aleppo, M. Antonelli, S. Gilardoni, F. Ragusa

Dipartimento di Fisica, Università di Milano e INFN Sezione di Milano, I-20133 Milano, Italy.

V. Büscher, H. Dietl, G. Ganis, K. Hüttmann, G. Lütjens, C. Mannert, W. Männer, H.-G. Moser, S. Schael, R. Settles, H. Seywerd, H. Stenzel, W. Wiedenmann, G. Wolf

Max-Planck-Institut für Physik, Werner-Heisenberg-Institut, D-80805 München, Germany[16]

P. Azzurri, J. Boucrot, O. Callot, S. Chen, M. Davier, L. Duflot, J.-F. Grivaz, Ph. Heusse, A. Jacholkowska,[1] M. Kado, J. Lefrançois, L. Serin, J.-J. Veillet, I. Videau,[1] J.-B. de Vivie de Régie, D. Zerwas

Laboratoire de l'Accélérateur Linéaire, Université de Paris-Sud, IN^{2}P^3-CNRS, F-91898 Orsay Cedex, France

G. Bagliesi, T. Boccali, C. Bozzi,[12] G. Calderini, R. Dell'Orso, I. Ferrante, A. Giassi, A. Gregorio, F. Ligabue, P.S. Marrocchesi, A. Messineo, F. Palla, G. Rizzo, G. Sanguinetti, G. Sguazzoni, R. Tenchini, A. Venturi, P.G. Verdini

Dipartimento di Fisica dell'Università, INFN Sezione di Pisa, e Scuola Normale Superiore, I-56010 Pisa, Italy

G.A. Blair, J. Coles, G. Cowan, M.G. Green, D.E. Hutchcroft, L.T. Jones, T. Medcalf, J.A. Strong

Department of Physics, Royal Holloway & Bedford New College, University of London, Surrey TW20 OEX, United Kingdom[10]

D.R. Botterill, R.W. Clifft, T.R. Edgecock, P.R. Norton, J.C. Thompson, I.R. Tomalin

Particle Physics Dept., Rutherford Appleton Laboratory, Chilton, Didcot, Oxon OX11 OQX, United Kingdom[10]

B. Bloch-Devaux, P. Colas, B. Fabbro, G. Faïf, E. Lançon, M.-C. Lemaire, E. Locci, P. Perez, J. Rander, J.-F. Renardy, A. Rosowsky, P. Saeger, A. Trabelsi,[21] B. Tuchming, B. Vallage

CEA, DAPNIA/Service de Physique des Particules, CE-Saclay, F-91191 Gif-sur-Yvette Cedex, France[17]

S.N. Black, J.H. Dann, C. Loomis, H.Y. Kim, N. Konstantinidis, A.M. Litke, M.A. McNeil, G. Taylor

Institute for Particle Physics, University of California at Santa Cruz, Santa Cruz, CA 95064, USA[22]

C.N. Booth, S. Cartwright, F. Combley, P.N. Hodgson, M. Lehto, L.F. Thompson

Department of Physics, University of Sheffield, Sheffield S3 7RH, United Kingdom[10]

K. Affholderbach, A. Böhrer, S. Brandt, C. Grupen, J. Hess, A. Misiejuk, G. Prange, U. Sieler
Fachbereich Physik, Universität Siegen, D-57068 Siegen, Germany[16]

G. Giannini, B. Gobbo
Dipartimento di Fisica, Università di Trieste e INFN Sezione di Trieste, I-34127 Trieste, Italy

J. Putz, J. Rothberg, S. Wasserbaech, R.W. Williams
Experimental Elementary Particle Physics, University of Washington, WA 98195 Seattle, U.S.A.

S.R. Armstrong, P. Elmer, D.P.S. Ferguson, Y. Gao, S. González, O.J. Hayes, H. Hu, S. Jin, J. Kile, P.A. McNamara III, J. Nielsen, W. Orejudos, Y.B. Pan, Y. Saadi, I.J. Scott, J. Walsh, J.H. von Wimmersperg-Toeller, Sau Lan Wu, X. Wu, G. Zobernig
Department of Physics, University of Wisconsin, Madison, WI 53706, USA[11]

[1]Also at CERN, 1211 Geneva 23, Switzerland.
[2]Now at Université de Lausanne, 1015 Lausanne, Switzerland.
[3]Also at Centro Siciliano di Fisica Nucleare e Struttura della Materia, INFN Sezione di Catania, 95129 Catania, Italy.
[4]Also Istituto di Fisica Generale, Università di Torino, 10125 Torino, Italy.
[5]Also Istituto di Cosmo-Geofisica del C.N.R., Torino, Italy.
[6]Supported by the Commission of the European Communities, contract ERBFMBICT982894.
[7]Supported by CICYT, Spain.
[8]Supported by the National Science Foundation of China.
[9]Supported by the Danish Natural Science Research Council.
[10]Supported by the UK Particle Physics and Astronomy Research Council.
[11]Supported by the US Department of Energy, grant DE-FG0295-ER40896.
[12]Now at INFN Sezione di Ferrara, 44100 Ferrara, Italy.
[13]Supported by the US Department of Energy, contract DE-FG05-92ER40742.
[14]Supported by the US Department of Energy, contract DE-FC05-85ER250000.
[15]Permanent address: Universitat de Barcelona, 08208 Barcelona, Spain.
[16]Supported by the Bundesministerium für Bildung, Wissenschaft, Forschung und Technologie, Germany.
[17]Supported by the Direction des Sciences de la Matière, C.E.A.
[18]Supported by Fonds zur Förderung der wissenschaftlichen Forschung, Austria.
[19]Now at SAP AG, 69185 Walldorf, Germany
[20]Now at Harvard University, Cambridge, MA 02138, U.S.A.
[21]Now at Département de Physique, Faculté des Sciences de Tunis, 1060 Le Belvédère, Tunisia.
[22]Supported by the US Department of Energy, grant DE-FG03-92ER40689.
[23]Now at LAL, 91898 Orsay, France.

1 Introduction

In this letter, a search for an invisibly decaying Higgs boson produced in association with a Z in the Higgs-strahlung process $e^+e^- \to hZ$, is presented. Such invisible decays are predicted in many extensions of the Standard Model [1]. The model dependence of the production rate can be embedded in the reduction factor ξ^2 with respect to the Standard Model production cross section.

Invisible Higgs boson decays have already been searched for in the data collected by ALEPH up to 184 GeV [2]. The events selected in the data were found to be compatible with the Standard Model expectations. Similar results have been obtained by DELPHI [3]. The search reported here is based on data collected by ALEPH in 1998 at a centre-of-mass energy of 188.6 GeV, with an integrated luminosity of 176.2 pb^{-1}.

2 The ALEPH detector

The ALEPH detector and its performance have been described in Refs. [4, 5, 6]. The tracking system consists of a silicon vertex detector, a cylindrical drift chamber and a large time projection chamber. A magnetic field of 1.5 T provided by a superconducting coil allows a charged particle $1/p_T$ relative resolution of $6 \times 10^{-4}\ p_T \oplus 5 \times 10^{-3}$ (p_T in GeV/c) to be achieved.

Electrons and photons are identified by using the information from the electromagnetic calorimeter, providing a measurement of their energy with a relative resolution of $0.18/\sqrt{E} + 0.009$ (E in GeV). The iron return yoke is instrumented and used as a hadronic calorimeter and, together with external chambers, allows muon identification. It provides a measurement of the hadronic energy with a relative resolution of $0.85/\sqrt{E}$. The coverage is rendered hermetic down to 34 mrad from the beam axis by two sets of luminosity calorimeters.

The information of all the subdetectors is combined in an *energy flow* algorithm which provides a list of *particles* used to determine the total energy with a resolution of $(0.6\sqrt{E} + 0.6)$ GeV and to form jets with a typical angular resolution of 20 mrad both in azimuthal and polar angles.

3 Event selection

Two selections addressing the $h\ell^+\ell^-$ (where ℓ denotes an electron or a muon) and the $hq\overline{q}$ final states have been developed to search for an invisibly decaying Higgs boson. The selection of the leptonic final state is essentially identical to that applied to lower energy data [2]. In the $hq\overline{q}$ channel, a new selection based on neural networks has been developed. To perform these studies, signal topologies were simulated at several Higgs boson masses with the HZHA generator [7] and large Standard Model background Monte Carlo samples were generated as detailed in Ref. [2].

The selection criteria were optimized by minimization of the expected 95% C.L. cross section upper limit in the absence of signal, as determined from Monte Carlo simulations (the $\overline{N}_{95}$ prescription [8]). In the optimization procedure, following the prescription

advocated in Ref. [9], the irreducible background coming from ZZ production was fully subtracted, but only 80% of the other backgrounds. However, to derive the final results, all backgrounds were fully subtracted, with systematic uncertainties taken into account as prescribed in Ref. [10].

In the following, unless otherwise specified, all efficiency and background values, and all numbers in general, pertain to the analysis designed for a 95 GeV/c^2 signal mass hypothesis.

3.1 The acoplanar lepton pair topology

The event selection of the search for an acoplanar pair of electrons or muons described in Ref. [2] is reoptimized for the sensitivity expected from the new data.

Events with two charged particles identified as electrons or muons of opposite charge and with polar angles $\theta_{1,2}$ such that $|\cos\theta_{1,2}| < 0.95$ are selected. The acollinearity must exceed 125°, the acoplanarity is required to be smaller than 178°, and the visible energy must be less than 65% of the centre-of-mass energy. Finally, the missing transverse momentum is required to be larger than 10 GeV/c.

From the measured momenta of the two leptons and their error estimates, a χ^2 measuring the consistency of the lepton pair mass with the Z mass is minimized. Events with a χ^2 greater than 5.0 are rejected.

The signal efficiency is 33%, corresponding to 0.7 signal events expected, while 4.5 events are expected from the background (2.5 WW, 1.4 ZZ, 0.4 $\tau^+\tau^-$, 0.2 e^+e^- and $\mu^+\mu^-$). Five events were selected in the data.

The systematic uncertainty on the efficiency was estimated to be 6% (relative), dominated by the limited Monte Carlo statistics, the lepton identification and tracking resolution. The uncertainty on the background estimation is 8% (relative), dominated by lepton identification and tracking resolution.

3.2 The acoplanar jet pair topology

3.2.1 Event selection

The acoplanar jet pair topology closely resembles that which arises from the $e^+e^- \to H\nu\bar{\nu}$ reaction. The main differences with respect to the search for the standard $H\nu\bar{\nu}$ final state arise from the Z and Higgs boson exchanged rôles: the missing mass is now due to the Higgs boson, and the visible mass to the Z. Furthermore, b-tagging is less powerful than for the standard search, but nevertheless allows some additional efficiency to be gained when the Z decays into $b\overline{b}$.

Therefore, an approach largely inspired from one of those developed in Ref. [9] to search for the $H\nu\bar{\nu}$ final state is used here: the two most important backgrounds, $q\overline{q}(\gamma)$ and WW+Weν, are handled by dedicated Neural Networks (NNs). Since the selection is very similar to the "3-fold-NN" analysis described in Ref. [9], only the changes with respect to that analysis are detailed below.

At the preselection level, the missing mass cut is relaxed in order to remain efficient for low invisible Higgs boson masses: $\not{M} > 30$ GeV/c^2. The visible mass must be smaller than 120 GeV/c^2.

The $q\overline{q}(\gamma)$ background rejection is addressed by a 7-variable neural network (7V-NN) similar to the one of Ref. [9], but with the missing mass replaced by the visible mass.

After the preselection, ~ 405 events are expected from the WW background, most of them being from semi-leptonic final states involving τ leptons. The anti-WW preselection of Ref. [9] is first applied. To reject further those events where a W decays into $\tau\nu_\tau$, one-prong τ candidates are selected. To take into account τ decays involving π^0s, up to four photons within a cone of 10° around the direction of the charged particle track are clustered to it in increasing order of angular distance, as long as the total invariant mass of the cluster is smaller than 1.5 GeV/c^2. Tau candidates are required to have a momentum larger than 3 GeV/c. The isolation of a τ candidate is defined as the energy contained within a 30° cone around its direction, excluding the τ cluster energy. This isolation energy, the distribution of which is shown in Fig. 1, is required to exceed 5 GeV.

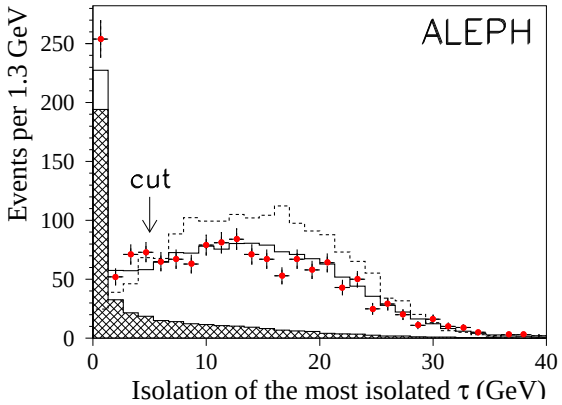

Figure 1: Distributions of the isolation of the most isolated τ for the background (open histogram) and the data (points with error bars) before the anti-WW preselection. The contribution due to the WW process is indicated (hatched histogram) and the signal distribution is also shown in arbitrary normalization (dashed histogram). The cut is indicated by an arrow.

As in Ref. [9], further rejection of the WW background is achieved using a 3-variable neural network (3V-NN), again with the missing mass replaced by the visible mass. Since in this analysis b-tagging cannot be used as in Ref. [9] to reject the Weν background, the 3V-NN is trained with an admixture of WW and Weν events.

The final selection criteria consist of requirements placed upon the rarities of the two neural networks, where the rarity of an event is defined as the fraction of signal events which are less signal like with respect to the considered variable. The distributions of the two NN rarities are shown in Fig. 2 for all backgrounds and for the data after all preselection cuts; the signal distributions are uniform by construction. A working point is determined, using the $\overline{N}_{95}$ prescription, by independently varying the cuts on both rarities. The cut values for this "general branch" are 0.30 and 0.29 for the 7V-NN and 3V-NN rarities, respectively.

As was already done in Ref. [2], one can further benefit from the fact that $\sim 22\%$ of the hadronic Z decays are into $b\overline{b}$ to apply looser cuts for well b-tagged events. Here, events are considered as well b-tagged if $\eta_1 + \eta_2$ is greater than 1.5, where $\eta_{1,2}$ are the b-tag NN outputs [11] for the two best tagged jets in the event. The cut values of 0.45 and 0.10 in

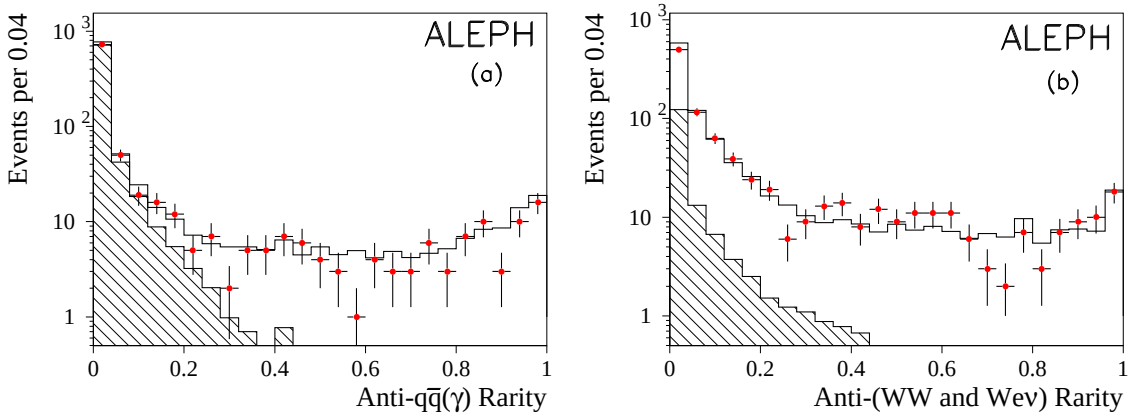

Figure 2: Distributions of the rarity of the anti-$q\bar{q}(\gamma)$ 7V-NN output (a) and of the rarity of the anti-(WW+Weν) 3V-NN output (b) for the background (histograms) and the data (points with error bars). Contributions from $q\bar{q}(\gamma)$ (a) and WW and Weν (b) events are indicated as hatched histograms.

this "b-tag branch" are determined in order to obtain the best performance for the "OR" of the two branches. The improvement achieved by adding the b-tag branch is marginal at high Higgs boson mass; however, it is significant for masses around 80 GeV/c^2 where the WW and Weν backgrounds dominate.

Finally, as in Ref. [9], a cut on E_{12}, the amount of energy detected within 12° of the beam axis, is applied. This cut principally addresses radiative $q\bar{q}$ events where a photon is detected at low angle. The cut value of 1% $\sqrt{s}$ was optimized taking into account the beam related background, based on the information from events triggered at random beam crossings. The inefficiency due to this cut is typically of the order of 1%.

At the working point, the signal efficiency is 38.6% (taking into account the systematic corrections discussed further down). This efficiency corresponds to 7.8 signal events, while 12.4 events are expected from standard background processes (8.0 ZZ, 0.9 WW, 1.5 Weν, 1.8 $q\bar{q}$ and 0.2 Z$\nu\bar{\nu}$). In the data, 14 events were selected.

In order to achieve a reasonably uniform performance in a wide mass range, neural networks were trained for various signal mass values (70, 75, 80, 85, 88, 90, 92 and 95 GeV/c^2), and the cuts on the rarities were optimized for each of those masses. This procedure effectively copes with the change of background composition when going from Higgs boson masses around 80 GeV/c^2, where the WW and Weν backgrounds dominate, to $\sim$ 90 GeV/c^2 where the ZZ background dominates. For mass values intermediate between those for which NNs were trained, interpolated cuts are applied on the interpolated rarities.

Altogether, a total of 44 events are observed, while 47.6 events are expected from Standard Model processes (taking into account the corrections discussed below). As shown in Fig. 3, a maximum of 23 events are selected for any given Higgs boson mass hypothesis.

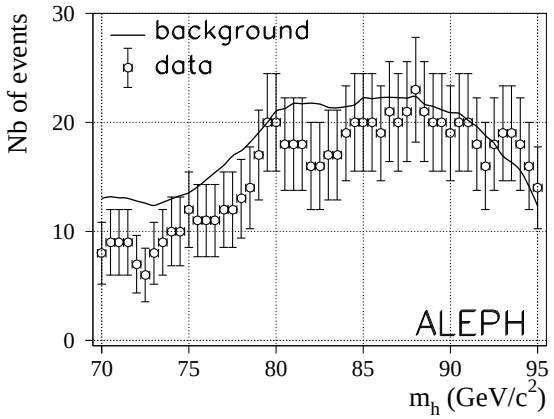

Figure 3: Expected number of events (solid line) and number of candidate events (points with error bars) as a function of the Higgs boson mass.

3.2.2 Systematic studies

Systematic effects related to the energy resolution and calibration and to the jet direction reconstruction have been studied using hadronic events collected at the Z peak in 1998. Except for the fact that no flavour selection is performed, the procedure is identical to the one described in Ref. [9]. As a result, the efficiencies for the signal — and for the irreducible ZZ and Z$\nu\bar{\nu}$ backgrounds — are reduced by 1% to 2% (relative), depending on the mass hypothesis. The simulation of the anti-WW preselection variables has also been studied with the Z peak data sample, resulting in efficiency reductions smaller than 0.2 % (relative). Half of these corrections are taken as systematic uncertainties.

The Weν cross section computed with PYTHIA is 20% larger than the value obtained with GRACE4f [12]. Since the latter generator is expected to produce a more accurate result for this cross section, the amount of Weν background is corrected accordingly, and half of this correction is taken as systematic uncertainty.

The remaining $q\bar{q}$ background, initially estimated with PYTHIA, is dominated by double radiative events. A study using the KORALZ generator, which is expected to simulate the initial state radiation more accurately, indicates that PYTHIA underestimates this background (by almost a factor three for the 95 GeV/c^2 mass hypothesis). A correction is therefore applied accordingly to the $q\bar{q}$ background estimate, and half of this correction is taken as systematic uncertainty.

To check further the WW and the modified Weν Monte Carlo predictions in the signal region, a sample of data events enriched in WW and Weν events is selected. For this purpose, the nominal cut on the 7V-NN output is applied to reject most of the $q\bar{q}$ events remaining after the preselections. About 87 events are expected from the standard processes, among which 42 and 24 originate from WW and Weν, respectively, while 77 events are selected in the data. Subtracting from both the observed and expected numbers of events the contribution from the other (mostly ZZ) backgrounds, the observed deficit in the data leads to a correction factor of 0.8 ± 0.1, where the error is dominated by the size of the data sample. Given the limited statistics, this correction is assumed to be constant over the whole range of 3V-NN outputs.

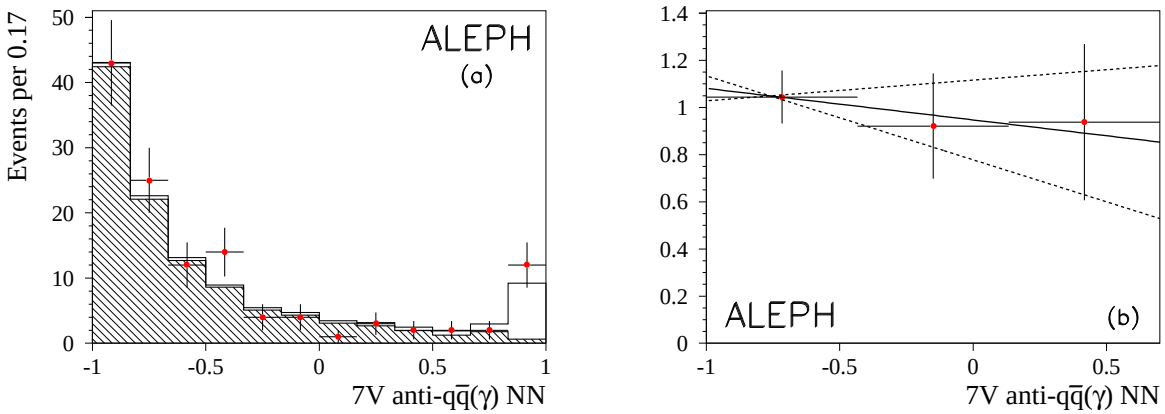

Figure 4: Distribution of the anti-$q\bar{q}(\gamma)$ 7V-NN for the background (histogram, with the $q\bar{q}(\gamma)$ contribution shown hatched) and the data (points with error bars) (a) and their ratio (b). The linear fit to this ratio is also shown, together with the lines corresponding to one standard deviation from this fit.

A similar procedure is used for the $q\bar{q}$ background. A data sample enriched in double radiative events (which constitute the bulk of the ultimate $q\bar{q}$ background) is selected by applying the nominal cut on the 3V-NN output, after all preselections. A total of 124 events are observed in the data, while 121 are expected from the simulation, among which 105 are double radiative events. The distribution of the 7V-NN output for these events is shown in Fig. 4(a). The $q\bar{q}$ background level in the signal region is determined from a linear fit to the data/Monte Carlo ratio for values of the 7V-NN output smaller than 0.7 (corresponding to the nominal rarity cut), as shown in Fig. 4(b). Extrapolating the result of the fit into the signal region (*i.e.*, to 7V-NN output values larger than 0.7), the correction factor is determined to be 0.83 ± 0.35, where the error is dominated by the data statistics.

4 Combined results

Overall, a total of 49 events are selected, combining the leptonic and hadronic channels, in agreement with the 52.1 events expected from all Standard Model background processes. The distributions of the Higgs boson mass, reconstructed with the Z mass constraint applied to the visible system, are shown in Fig. 5 for both the leptonic and hadronic channels.

The combined observed and expected confidence levels are shown in Fig. 6(a). The confidence levels for background only are shown in Fig. 6(b). These confidence levels have been calculated using the reconstructed mass as discriminating variable with the same statistical procedure as in Ref. [9, 13]. For Higgs bosons produced with the Standard Model cross section and decaying invisibly, the expected 95% CL limit is 94.4 GeV/c^2. The mass lower limit obtained is 95.4 GeV/c^2.

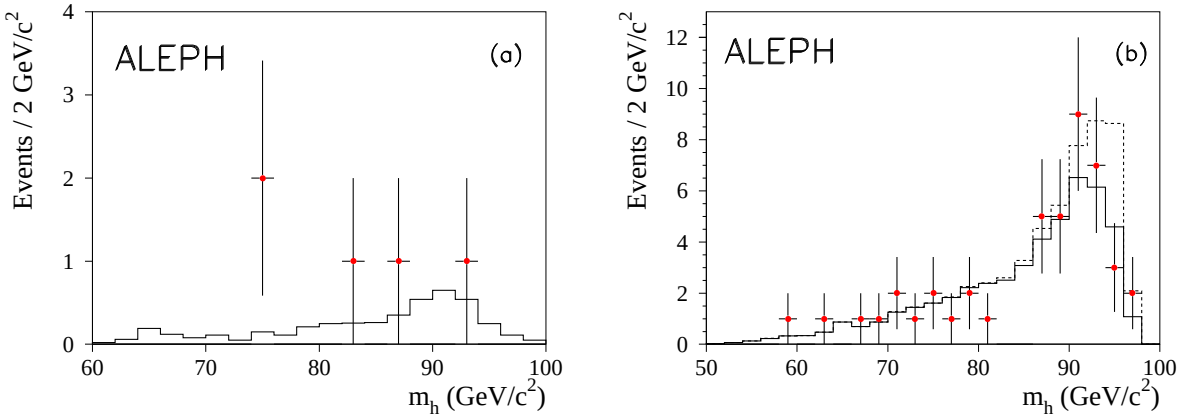

Figure 5: Distribution of the reconstructed Higgs boson mass in the leptonic (a) and hadronic (b) channels for the data (points with error bars) and for the background (full histograms). The contribution of a 95 GeV/c^2 mass Higgs boson signal is also shown for the hadronic channel (dashed histogram).

The result of this analysis can alternatively be presented as an exclusion domain in the (m_{h}, ξ^2) plane, as shown in Fig. 7. Here ξ^2 is to be interpreted as the product of the cross section reduction factor with respect to the Standard Model and of the branching ratio into invisible final states.

5 Conclusions

Searches for invisible decay modes of the Higgs boson produced in the reaction $\mathrm{e^+e^-} \to \mathrm{hZ}$ have been carried out in the acoplanar jet and acoplanar lepton topologies using 176.2 pb^{-1} of data collected by ALEPH at a centre-of-mass energy of 188.6 GeV. No excess with respect to the Standard Model has been found in the data, yielding a lower limit of 95.4 GeV/c^2 for the mass of an invisibly decaying Higgs boson produced with a cross section equal to that of the Standard Model Higgs boson.

Acknowledgements

We wish to thank our colleagues from the accelerator divisions for the successful operation of LEP at high energy. We are indebted to the engineers and technicians in all our institutions for their contribution to the excellent performance of ALEPH. Those of us from non-member states thank CERN for its hospitality.

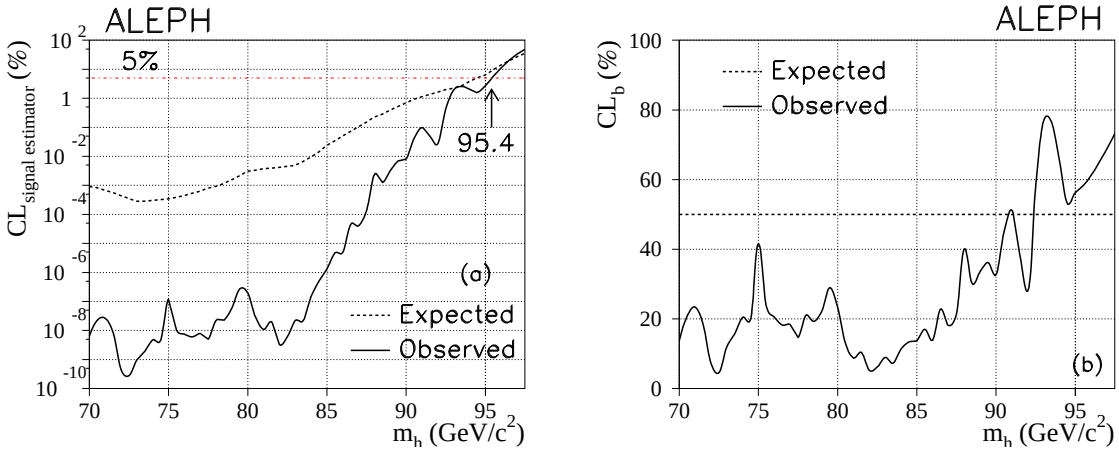

Figure 6: Signal estimator confidence levels (a) for the combination of the leptonic and hadronic channels. The confidence levels for background only are also displayed in (b).

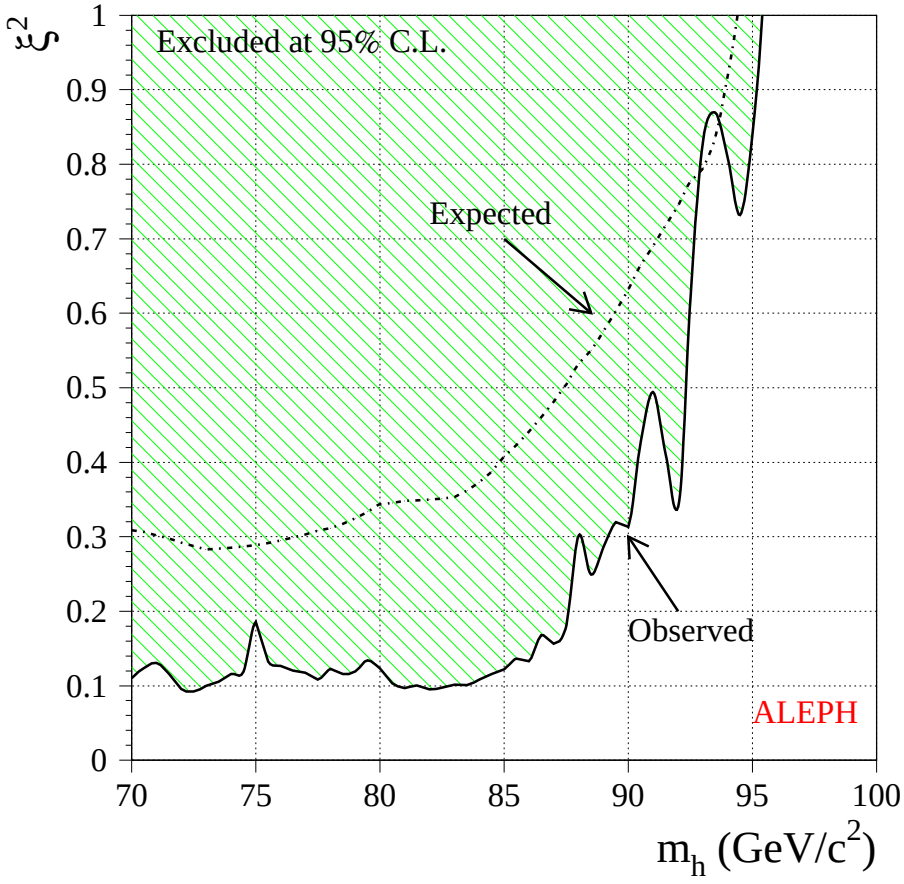

Figure 7: Excluded region at the 95% C.L. in the (m_{h}, ξ^2) plane.

References

[1] For reviews, see:
M. Carena and P.M. Zerwas (Conveners) *et al.* in "Higgs physics at LEP2", Ed: G. Altarelli, T. Sjöstrand, and F. Zwirner, CERN-96-01 (1996) 351;
S. P. Martin and J. D. Wells, *"Motivation and detectability of an invisibly-decaying Higgs boson at the Fermilab Tevatron"*, hep-ph/9903259.

[2] The ALEPH Collaboration, *"Search for invisible Higgs boson decays in e^+e^- collisions at centre-of-mass energies up to 184 GeV"*, *Phys. Lett.* **B450** (1999) 301.

[3] The DELPHI Collaboration, *"A search for invisible Higgs bosons produced in e^+e^- interactions at LEP2 energies"*, CERN-EP/99-059, to be published in *Phys. Lett. B.*

[4] The ALEPH Collaboration, *"ALEPH: a detector for electron-positron annihilations at LEP"*, *Nucl. Instrum. Methods* **A294** (1990) 121.

[5] D. Creanza *et al.*, *Nucl. Instrum. Methods* **A409** (1998) 157.

[6] The ALEPH Collaboration, *"Performance of the ALEPH detector at LEP"*, *Nucl. Instrum. Methods* **A360** (1995) 481.

[7] P. Janot, "The HZHA generator", in Physics at LEP 2, Eds. G. Altarelli, T. Sjöstrand and F. Zwirner, CERN 96-01 (1996) 309.

[8] J.-F. Grivaz and F. Le Diberder, *"Complementary analyses and acceptance optimization in new particle searches"*, LAL-92-37.

[9] The ALEPH Collaboration, *"Search for the neutral Higgs Bosons of the Standard Model and the MSSM in e^+e^- collisions at $\sqrt{s} = 188.6$ GeV"*, ALEPH 99-053, CONF 99-029, submitted to the HEP99 Conference, Tampere, Finland, Abstract 7-428.

[10] R. D. Cousins and W. L. Highland, *Nucl. Instrum. Methods* **A320** (1992) 331.

[11] The ALEPH Collaboration, *"Search for the neutral Higgs bosons of the MSSM in e^+e^- collisions at $\sqrt{s}$ from 130 to 172 GeV"*, *Phys. Lett.* **B412** (1997) 173.

[12] J. Fujimoto *et al.*, *Comput. Phys. Commun.* **100** (1997) 128.

[13] S. Jin and P. McNamara, *"The Signal Estimator Limit Setting Method"*, physics/9812030;
H. Hu and J. Nielsen, *"Analytic Confidence Level Calculations using the Likelihood Ratio and Fourier Transform"*, physics/9906010.